Thermoelectric figure of merit of Bi/Pb$_{1-x}$Eu$_x$Te superlattices

T. Koga[1,*] and O. Rabin[2]

[1]*Division of Engineering and Applied Sciences, Harvard University, Cambridge, Massachusetts 02138*
[2]*Department of Chemistry, Massachusetts Institute of Technology, Cambridge, Massachusetts 02139*

M. S. Dresselhaus[†]

Department of Physics and Department of Electrical Engineering and Computer Science, Massachusetts Institute of Technology,
Cambridge, Massachusetts 02139

An enhanced thermoelectric figure of merit $Z_{3D}T$ is predicted for Bi/(111)Pb$_{1-x}$Eu$_x$Te superlattices. The values of $Z_{3D}T$ obtained for $x \approx 1$ superlattices are 2.31, 1.55, and 1.61 at 300, 150, and 77 K, respectively, showing that they are promising candidates for thermoelectric elements in the temperature range 77–300 K. Even with x as small as 0.1, where the conduction-band offset ΔE_c is estimated to be 0.25 eV, the predicted $Z_{3D}T$ values are 1.75, 1.16, and 1.18 at 300, 150, and 77 K, respectively. It is proposed that other families of Bi-based superlattices, such as Bi/(111)CdTe superlattices, should also be good candidates for low-temperature thermoelectric elements.

The use of superlattice structures to design useful thermoelectric materials with a large thermoelectric figure of merit ZT ($= S^2 \sigma T/\kappa$, where S, σ, κ, and T are the Seebeck coefficient, electrical conductivity, thermal conductivity, and absolute temperature, respectively) has attracted significant interest in the thermoelectric materials community.[1–16] The basic strategies for enhancing ZT using low-dimensional structures are based on (1) the use of an enhanced density of states for electrons (or holes) near the band edge to increase the magnitude of the Seebeck coefficient $|S|$ at a given carrier concentration and (2) the use of increased boundary scattering of phonons at the quantum well-barrier interfaces in the superlattice to reduce the lattice thermal conductivity κ_{ph} relative to the bulk values.[11,16] Recently, the original proposal by Hicks *et al.*[7,11,13,16] has been extended to more realistic systems, such as GaAs/AlAs (Refs. 1–3) and Si/Ge (Refs. 1,4) short-period superlattices, and an enhanced three-dimensional figure of merit ($Z_{3D}T$) for the whole superlattice was predicted relative to the ZT's for the corresponding bulk materials.

The key strategy for the successful design of thermoelectric materials using a superlattice structure is to find materials with highly anisotropic constant energy surfaces for the quantum well layers and materials for the barrier layers that are chemically (and structurally) compatible with the quantum well material and have large values for the energy band gaps to provide sufficient conduction- and valence-band offsets for the superlattices. Bismuth (Bi) is a semimetal that has various unique properties, such as a highly anisotropic Fermi surface, large electron and hole mobilities, and a small lattice thermal conductivity.[17–21] These features of Bi make it potentially a very desirable material for thermoelectric applications, especially in its semiconducting form.[7,8,17] A semimetal-semiconductor transition in Bi has been predicted and experimentally demonstrated using low-dimensional structures, such as quantum wells and wires.[22–25] The two-dimensional nature of the electron transport in Bi/(111)PbTe superlattices has also been reported experimentally.[26–28]

Here we report a theoretical investigation of the thermoelectric properties of Bi/(111)Pb$_{1-x}$Eu$_x$Te superlattices. We choose Pb$_{1-x}$Eu$_x$Te alloys for the barrier layer material for the Bi quantum wells because (1) the Bi hexagonal (001) plane has good lattice matching with the Pb$_{1-x}$Eu$_x$Te cubic (111) plane [lattice mismatch $\sim 0.3\%$ and $\sim 2\%$ for (001)Bi/(111)PbTe and (001)Bi/(111)EuTe interfaces, respectively], (2) Bi/(111)PbTe superlattices have already been fabricated,[26–28] and there are good prospects that Bi/(111)Pb$_{1-x}$Eu$_x$Te superlattices will be grown in the near future, and (3) the ability to change the energy band gap between 0.32 eV (PbTe) and 2.2 eV (EuTe) continuously (by changing the value of x) provides us with a large controllability in materials design when and if this material reaches the stage of actual superlattice fabrication for thermoelectric applications. The first and simplified approach to modeling this superlattice system, presented below, is intended to estimate its prospect as a thermoelectric material in the temperature range 77–300 K and to guide further experimental and theoretical efforts.

The calculation of $Z_{2D}T$ for isolated quantum wells of Bi has been reported elsewhere.[7,8] Extension of this model is made here to include the effects of finite barrier width and finite barrier height (Kronig-Penney model),[29] and to include the opposite sign for the electron and hole contributions to the thermoelectric transport (two-band, two-carrier model). For simplicity, we assume a parabolic energy dispersion relation for all electron and hole pockets. For the barrier layer, the effective mass tensor component perpendicular to the planes of the superlattice $m_\perp$ has the values of $0.0372m$ (for an oblique valley coupled to the L valleys in Bi) and $0.425m$ (for a longitudinal valley coupled to the T valley in Bi), for electrons and holes, respectively. In the bismuth layer, the effective mass tensor for the electron pockets is given by $m_e^x = 0.00651m$, $m_e^y = 1.362m$, and $m_e^z = 0.0101m$, where the x, y, and z axes are taken to be parallel to the principal axes of the constant energy ellipsoid, and the effective mass tensor for the holes is given by $m_h^{x,y} = 0.0644m$, $m_h^z = 0.696m$.[18]
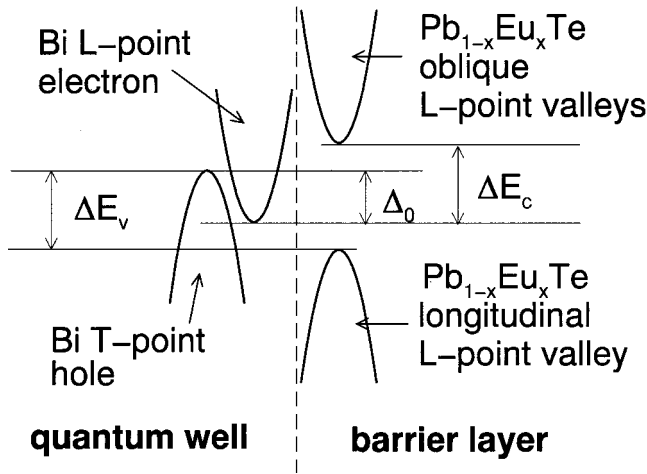
PRB <u>62</u>   16 703

FIG. 1. Conduction- and valence-band offset diagram for Bi/(111)Pb$_{1-x}$Eu$_x$Te superlattices. Bi L-point conduction valleys are assumed to be coupled with the oblique L-point conduction-band valleys of Pb$_{1-x}$Eu$_x$Te, whereas the Bi T-point valence-band valley is assumed to be coupled with the longitudinal L-point valence-band valley of Pb$_{1-x}$Eu$_x$Te. Here $\Delta E_c = \Delta E_v$ is assumed in the present work.

In reality, the electronic energy dispersion at the L points for bulk Bi is highly nonparabolic and temperature dependent.[19,20] However, at the optimal structure of the superlattice, the energy for the lowest conduction subband edge is always higher than the Fermi energy of bulk Bi ($E_F^e = 23$ meV), and in this energy range the mass variations with respect to energy and temperature are relatively weak. Therefore, the values given above, which correspond to the effective mass tensor at the Fermi energy of bulk bismuth at low temperatures, are a conservative approximation for the values of the effective mass tensor components of the lowest conduction subband of the superlattice.

The carrier mobility values for bulk Bi and their temperature dependence[17] are used in the model calculations reported here. Experimental work on Bi films and superlattices[24] has shown that the mobilities are affected by the layer thickness, suggesting a linear dependence on film thickness. However, there is no clear evidence whether these observations are intrinsic to the Bi/semiconductor interface (present even at a perfectly structured boundary), or rather result from the difficulty of fabricating good quality superlattices and interfaces as the layer thicknesses decrease. Particularly, the unintentional p-type doping observed in the samples[24,28,30] is consistent with the presence of defects or the interdiffusion of atoms between the layers. Experiments in PbTe/PbEuTe superlattices indicate that the mobilities of the quantum wells should not differ significantly from those of the bulk.[12]

The temperature dependence of the band overlap energy Δ_0 for bulk Bi (see Fig. 1) is also considered.[17] We assume that the conduction- and valence-band offsets, denoted by ΔE_c and ΔE_v, respectively (as defined in Fig. 1), are obtained by equally splitting the difference in the energy band gaps between Bi and Pb$_{1-x}$Eu$_x$Te, since there is no prior literature available on ΔE_c and ΔE_v in this system. This leads to a model of a type-I superlattice, in which the extrema of both the valence band and the conduction band are
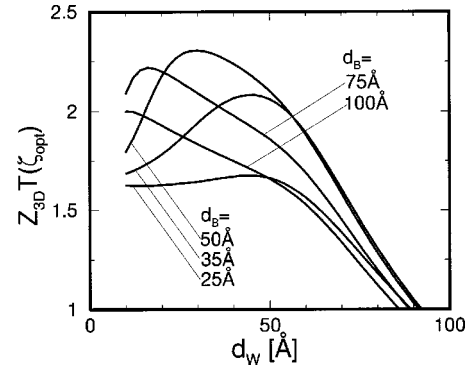

FIG. 2. Calculated thermoelectric figure of merit at the optimum carrier concentration $Z_{3D}T(\zeta_{opt})$ as a function of the well (Bi) and barrier (Pb$_{1-x}$Eu$_x$Te) thicknesses (denoted by d_W and d_B, respectively) at 300 K. The conduction- and valence-band offsets are taken to be 1 eV (corresponding to $x \approx 1$).

located in the Bi layers. Appropriate adjustments of the model would have to be made, however, as experimental results accumulate, particularly if it were found that the alignment of the band offsets for some range of x is of a type-II superlattice.

The lattice thermal conductivity κ_{ph} used in the calculation is determined by using κ_{ph} values for bulk Bi and bulk PbTe. We choose an average value between these ($\kappa_{ph} = 1.5$ W/m K) as an upper-limit estimate for κ_{ph} for Bi/(111)Pb$_{1-x}$Eu$_x$Te superlattices at 300 K. The actual values for κ_{ph} for the Bi/(111)Pb$_{1-x}$Eu$_x$Te superlattices should be smaller than $\kappa_{ph} = 1.5$ W/m K, due to the alloy scattering and the boundary scattering of phonons at the Bi/(111)Pb$_{1-x}$Eu$_x$Te interfaces. We also assume that κ_{ph} for the Bi/(111)Pb$_{1-x}$Eu$_x$Te superlattices obeys a T^{-1} temperature dependence, unless the phonon mean free path l is limited by the boundary scattering of phonons ($l \approx d_W, d_B$). We take the value of κ_{ph} to be independent of temperature for $T < T_l$, the threshold temperature T_l below which l is limited by the boundary scattering of phonons, truncated by the layer thicknesses. In the present Bi/(111)Pb$_{1-x}$Eu$_x$Te superlattices, T_l is calculated to be approximately 150 K.

Shown in Fig. 2 are the calculated $Z_{3D}T$ values at the optimum carrier concentration for the n-type Bi/(111)Pb$_{1-x}$Eu$_x$Te superlattices [denoted by $Z_{3D}T(\zeta_{opt})$] as a function of quantum well (Bi) and barrier (Pb$_{1-x}$Eu$_x$Te) layer thicknesses (denoted by d_W and d_B, respectively). Explicit calculations are made for $x \approx 1$, $\Delta E_c = \Delta E_v = 1$ eV, and $\Delta_0 = 104.2$ meV at 300 K (see Fig. 1). For most of the values of d_B considered in Fig. 2, we observe that $Z_{3D}T(\zeta_{opt})$ first increases with decreasing d_W, reaches a maximum at a certain value for d_W (denoted as $d_{W|opt}$), and then decreases as d_W is further decreased. The first increase in $Z_{3D}T(\zeta_{opt})$ is due to the increased density of states for electrons [the height of the steps in the electronic density of states is proportional to $(d_W + d_B)^{-1}$] and due to the elimination of the holes with the formation of the quantum confinement induced band gap in bismuth. The decrease in $Z_{3D}T(\zeta_{opt})$ below $d_W = d_{W|opt}$ is due to the increased tunneling of electrons between the Bi layers across the barrier regions. The highest value for $Z_{3D}T[Z_{3D}T(\zeta_{opt}) = 2.31]$ for this condition is obtained for $d_B = 50$ Å and $d_{W|opt} = 30$ Å at a carrier concentration of
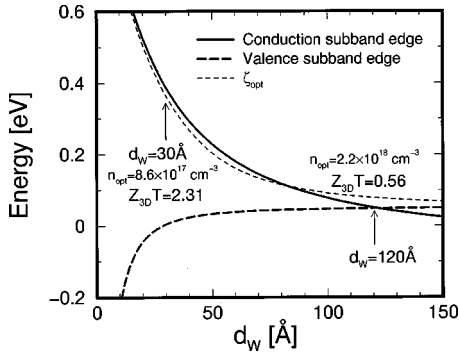
FIG. 3. Relative energies for the conduction (solid curve) and valence (long-dashed curve) subband edges as a function of quantum well thickness d_W for Bi/(111)Pb$_{1-x}$Eu$_x$Te superlattices ($x \approx 1$) at 300 K. The conduction- and valence-band offsets and the barrier layer thickness d_B are taken to be 1 eV (see text) and 50 Å, respectively. The zero energy in the figure is the midpoint in the overlap energy ($\Delta_0 = 104$ meV at 300 K) between the conduction and valence bands for bulk Bi.

TABLE I. Optimum structures and calculated $Z_{3D}T$'s for Bi/(111)Pb$_{1-x}$Eu$_x$Te superlattices.

T [K]	d_W [Å]	d_B [Å]	n_{opt} [cm^{-3}]	$Z_{3D}T$
$\Delta E_c = 1.0$ eV ($x \approx 1$)				
300	30	50	8.6×10^{17}	2.31
150	30	60	5.9×10^{17}	1.55
77	28	75	2.6×10^{17}	1.61
$\Delta E_c = 0.5$ eV ($x \approx 0.3$)				
300	26	75	7.9×10^{17}	2.03
150	36	75	5.1×10^{17}	1.34
77	40	85	2.4×10^{17}	1.37
$\Delta E_c = 0.25$ eV ($x \approx 0.1$)				
300	18	85	7.7×10^{17}	1.75
150	36	100	4.7×10^{17}	1.16
77	50	105	2.2×10^{17}	1.18

8.6×10^{17} cm^{-3} (see Fig. 3). It is noted that for the values of d_W near $d_{W|opt}$, Bi/(111)Pb$_{1-x}$Eu$_x$Te superlattices are always semiconducting (for all values of d_B that are considered here). For example, the band edge energies as a function of quantum well thickness are shown in Fig. 3 for $d_B \approx 50$ Å. Even for $d_W \approx 70$ Å, where the holes in the valence band start to push the optimum chemical potential ζ_{opt} up into the conduction band, the band gap energy for the superlattice is several times as large as the thermal energy ($E_g = 103$ meV, whereas $k_B T = 26$ meV at 300 K). For n-type superlattices with $d_W < 60$ Å, the contribution of holes to the total thermoelectric transport is negligible.

We have also investigated the optimum structures and doping levels that give the largest values for $Z_{3D}T$ at various temperatures (77, 150, and 300 K) and for various values of the conduction band offset ($\Delta E_c = 0.25, 0.5$, and 1.0 eV). The investigation and prediction of the materials with enhanced values for $Z_{3D}T$ at low temperatures ($T < 150$ K) are important because there are virtually no thermoelectric materials at present that are useful at low temperatures, where there exist strong demands for thermoelectric refrigerators to cool high-T_c superconductors. The results for these calculations for $Z_{3D}T$ are summarized in Table I.

As progress is made in the fabrication of Bi/Pb$_{1-x}$Eu$_x$Te superlattices, the computational model presented here would need further refinement. When comparing theoretical predictions with experimental data from specific samples, special attention should be given to the effect of strain on the trans-

port properties. Strain accommodates the lattice mismatch between Bi and Pb$_{1-x}$Eu$_x$Te (Ref. 27) and is controllable to some extent by the choice of substrate, buffer layer, and layer thicknesses. The strain is expected to be more significant with increasing concentrations of Eu in the barrier layer due to the increase in the lattice mismatch. Of great importance to accurate modeling are also the nature of scattering processes in specific samples, the sources of unintentional doping, and the values of the band offsets, all of which might have a large impact on the optimal $Z_{3D}T$ values.

In summary, an enhanced thermoelectric figure of merit $Z_{3D}T$ is predicted for n-type Bi/(111)Pb$_{1-x}$Eu$_x$Te superlattices at optimal doping concentrations. The values of $Z_{3D}T$ for $x \approx 1$ superlattices are predicted to be 2.31, 1.55, and 1.61 at 300, 150, and 77 K, respectively. These values for $Z_{3D}T$ and the optimum structural design for the superlattice are found to depend on the conduction-band offset ΔE_c. It is proposed that Bi/(111)Pb$_{1-x}$Eu$_x$Te superlattices should be a promising candidate for thermoelectric elements at low temperatures. Other families of Bi quantum well superlattices, such as Bi/(111)CdTe superlattices,[24,30] should also show similar thermoelectric properties at low temperatures.

*Present address: NTT Basic Research Laboratories, 3-1 Morinosato-Wakamiya, Atsugi-city, Kanagawa, 243-0198, Japan.

†On leave from Department of Physics and Department of Electrical Engineering and Computer Science, Massachusetts Institute of Technology, Cambridge, Massachusetts, 02139.

[1] T. Koga, X. Sun, S.B. Cronin, and M.S. Dresselhaus, in *The 18th International Conference on Thermoelectrics: ICT Symposium Proceedings, Baltimore* (Institute of Electrical and Electronics Engineers, Piscataway, NJ, 1999).

[2] T. Koga, X. Sun, S.B. Cronin, M.S. Dresselhaus, K.L. Wang, and G. Chen, J. Comput.-Aided Mater. Design **4**, 175 (1997).

[3] T. Koga, X. Sun, S.B. Cronin, and M.S. Dresselhaus, Appl. Phys. Lett. **73**, 2950 (1998).

[4] T. Koga, X. Sun, S.B. Cronin, and M.S. Dresselhaus, Appl. Phys. Lett. **75**, 2438 (1999); T. Koga, S. B. Cronin, M. S. Dresselhaus, J. L. Lin, and K. L. Wang, Appl. Phys. Lett. **77**, 1490 (2000).

[5] D.A. Broido and T.L. Reinecke, Appl. Phys. Lett. **70**, 2834 (1997).

[6] D.A. Broido and T.L. Reinecke, Phys. Rev. B **51**, 13 797 (1995).

[7] L.D. Hicks, T.C. Harman, and M.S. Dresselhaus, Appl. Phys. Lett. **63**, 3230 (1993).

[8] D.A. Broido and T.L. Reinecke, Appl. Phys. Lett. **67**, 1170 (1995).

[9] P.J. Lin-Chung and T.L. Reinecke, Phys. Rev. B **51**, 13 244 (1995).

[10] J.O. Sofo and G.D. Mahan, Appl. Phys. Lett. **65**, 2690 (1994).

[11] L.D. Hicks and M.S. Dresselhaus, Phys. Rev. B **47**, 12 727 (1993).

[12] T.C. Harman, D.L. Spears, and M.J. Manfra, J. Electron. Mater. **25**, 1121 (1996).

[13] L.D. Hicks, T.C. Harman, X. Sun, and M.S. Dresselhaus, Phys. Rev. B **53**, R10 493 (1996).

[14] T. Koga, S.B. Cronin, T.C. Harman, X. Sun, and M.S. Dresselhaus, in *Semiconductor Process and Device Performance Modeling*, edited by J.S. Nelson, C.D. Wilson, and S.T. Dunham, Mater. Res. Soc. Symp. Proceedings No. **490** (Materials Research Society, Pittsburgh, 1998), p. 263.

[15] T. Koga, T.C. Harman, S.B. Cronin, and M.S. Dresselhaus, Phys. Rev. B **60**, 14 286 (1999).

[16] L.D. Hicks and M.S. Dresselhaus, Phys. Rev. B **47**, 16 631 (1993).

[17] C.F. Gallo, B.S. Chandrasekhar, and P.H. Sutter, J. Appl. Phys. **34**, 144 (1963).

[18] R.T. Isaacson and G.A. Williams, Phys. Rev. **185**, 682 (1969).

[19] M.P. Vecchi and M.S. Dresselhaus, Phys. Rev. B **10**, 771 (1974).

[20] J. Heremans and O.P. Hansen, J. Phys. C **12**, 3483 (1979).

[21] X. Sun, Ph.D. thesis, Massachusetts Institute of Technology, 1999.

[22] Z. Zhang, J.Y. Ying, and M.S. Dresselhaus, J. Mater. Res. **13**, 1745 (1998).

[23] Z. Zhang, X. Sun, M.S. Dresselhaus, J.Y. Ying, and J.P. Heremans, Appl. Phys. Lett. **73**, 1589 (1998).

[24] C.A. Hoffman, J.R. Meyer, F.J. Bartoli, A. Di Venere, X.J. Yi, C.L. Hou, H.C. Wang, J.B. Ketterson, and G.K. Wong, Phys. Rev. B **48**, 11 431 (1993), and references therein.

[25] M. Lu, R.J. Zieve, A. van Hulst, H.M. Jaeger, T.F. Rosenbaum, and S. Radelaar, Phys. Rev. B **53**, 1609 (1996).

[26] S.-C. Shin, J.B. Ketterson, and J.E. Hilliard, Phys. Rev. B **30**, 4099 (1984).

[27] S.-C. Shin, J.E. Hilliard, and J.B. Ketterson, Thin Solid Films **111**, 323 (1984).

[28] S.-C. Shin, J.E. Hilliard, and J.B. Ketterson, J. Vac. Sci. Technol. A **2**, 296 (1984).

[29] C. Kittel, *Introduction to Solid State Physics*, 7th ed. (Wiley, New York, 1996), p. 180.

[30] S. Cho, A. Di Venere, G.K. Wong, J.B. Ketterson, J.R. Meyer, and C.A. Hoffman, Solid State Commun. **102**, 673 (1997).